J Braz. Soc. Mech. Sci. Eng.
DOI 10.1007/s40430-016-0569-8

TECHNICAL PAPER

Energy consumption pattern modification in greenhouses by a hybrid solar–geothermal heating system

Ahmad Arabkoohsar[1] · Mahmood Farzaneh-Gord[2] · R. Ghezelbash[2] · Ricardo N. N. Koury[3]

Received: 27 January 2016 / Accepted: 17 May 2016

Abstract Greenhouses play a key role in producing various crops in Bohemian climates and during the entire year. To provide the desired temperature within the greenhouse during the cold months of the year, diesel air heaters are generally employed, burning huge amount of fossil fuels. In this work, an innovative hybrid system including solar and geothermal heating units has been proposed to be used to reduce the heating duty of diesel air heaters in greenhouses. Taking ambient temperature in different seasons and the desired temperature in the greenhouse into account, three operational strategies are planned for the proposed system. Next, considering the defined operational strategies and economic issues, the solar and geothermal parts are accurately sized and designed. Finally, a hybrid system including a solar system with 430 flat plate collectors and a geothermal system consisting of 35 boreholes, with 150 m depth each, is found to be the most thermo-economically efficient system for the case study of this work. A comprehensive energy analysis on the designed configuration shows that a total annual of almost 256,000 and 192,000 m^3 fuel saving may be possible in the case study by the solar and geothermal systems, respectively. Finally, the proposed hybrid system performance is economically compared with previously proposed systems for the same objective by the internal rate of return (IRR) method, proving its superiority with an IRR of 0.115.

Keywords Greenhouse · Geothermal energy · Solar energy · Multi-node storage tank · IRR

Technical Editor: Francis HR Franca.

✉ Ahmad Arabkoohsar
mani.koohsar@yahoo.com

[1] Department of Mechanical Engineering, Minoodasht Branch, Islamic Azad University, Minoodasht, Iran

[2] Faculty of Mechanical Engineering, Shahrood University of Technology, Shahrood, Iran

[3] Department of Mechanical Engineering, Universidade Federal de Minas Gerais (UFMG), Belo Horizonte, Brazil

Abbreviations

Nomenclature

A	Area (m^2)
c_p and c	Specific heat (kJ/kg.K)
C_n	Cash flow in each year ($)
D and d	Diameter (m)
D'	Ineffective borehole length (m)
FR	Removal factor
h	Enthalpy (kJ/kg)
H	Effective length of borehole (m)
I	Solar irradiation (W/m^2)
IRR	Internal rate of return
k	Thermal conductivity (W/m.K)
LHV	Lower heating value (kJ/kg)
L	Length (m)
m	Mass (kg)
$\dot{m}$	Mass flow rate (kg/s)
n	Number of years
N	Number of air exchanger per hour
NPV	Net present value ($)
N_{bh}	Number of boreholes
q	Heat transfer rate per unit length (kW/m)
$\dot{Q}$	Heat transfer rate (kW)
$r_{i,j}$	Radial distance between borehole i and j (m)
r	Internal rate of return
R	Thermal resistance (m^2.K/W)
S	Absorbed solar flux (W/m^2)

Published online: 02 June 2016

S'	Laplace transform variable
t	Time (s)
T	Temperature (ºC)
U	Overall heat transfer coefficient (W/m^2.K)
V	Greenhouse volume (m^3)

Greek symbols

β	Collector slope angle
β'	Shape factor
η	Efficiency
λ	Time step
α	Thermal diffusion coefficient (m^2/h)
$(\tau\alpha)_{av}$	Average transmission-emission factor of the collector

Subscriptions

am	Ambient
b	Beam
bh	Borehole
conv	Convection
cond	Conduction
d	Diffuse
f	Fluid in GHX
fuel	Fuel
GR	Greenhouse
gr	Ground
grt	Grout
GHX	Ground heat exchanger
h	Heater
i	Internal
in	Inlet
lost	Heat lost
ls	Line source
o	External
out	Outlet
p	Pipe
st	Storage tank
u	Useful heat gained through the collector
vent	Ventilation
w	Water

1 Introduction

Greenhouses are used to cultivate vegetables, fruits and flowers. They are more efficient than traditional approaches and may be used for cultivation year-round and even in bohemian climates employing solar irradiation. The intensity of energy usage in greenhouses has been studied by many authors generally [1, 2] and even for specific crops (tomato [3, 4], grape [5], and strawberry [6]). All the aforementioned studies demonstrated the excessive amount of energy consumption in the greenhouses. The researches show that in spite of the significant amount of solar energy absorbed into the greenhouses by passive solar system, a huge amount of fuel is still needed for reaching the desirable temperature of crop on many days over the year. Currently, the heating demand of greenhouses is provided by diesel air heaters which burn natural gas as the main fuel in Iran (and probably other countries). Many studies have been done to find opportunities and methods to decrease the amount of fuel consumption in greenhouses, resulting in numerous proposals aimed at improving the thermal behavior of greenhouses such as more efficient cover materials, better framework shapes [7, 8] and many others focused on employing active solar or geothermal systems for providing the greenhouses heating demand [9–15].

In terms of employing renewable energy sources, Rafferty [16] studied the feasibility of employing geothermal energy in greenhouses for the first time. Bakos et al. [17] analyzed an extended heating system which used low-temperature water or direct geothermal fluid to heat a greenhouse. Karytsas et al. [18] evaluated low-enthalpy heating employing geothermal heat in greenhouses in various parts of the world. Ghosal and Tiwari [19] also presented a mathematical modeling for geothermal-based greenhouse heating systems. On the other hand, Willits et al. [11] presented the first study related to employing active solar systems in greenhouses by proposing a solar energy storage system in them. Zabeltitz [20], later, proposed employing solar energy for heating greenhouses in different ways, namely, separate solar collectors, solar collectors integrated in greenhouse and the use of greenhouse itself as a solar collector. In another work, solar energy rock-bed storage was proposed to provide the heating demand of greenhouses [21]. Li et al. [22] investigated the performance of a solar heating system with underground seasonal energy storage for greenhouses. In one of the last studies in this area, Farzaneh-Gord et al. [23] presented another approach of solar energy storage in greenhouses by evaluating the energy performance of a greenhouse in Iran as the case study.

This work, however, presents an innovative system taking advantage of solar energy as well as low-temperature geothermal energy to improve the greenhouse energy performance. To the authors' knowledge, this is the first time that a combination of active solar and geothermal systems, simultaneously, in greenhouses is proposed. By such a system, not only the initial investment of the heating system decreases significantly due to the considerably low capital cost of low-temperature geothermal heating system, but also the desired temperature could be achieved by the solar heating system. Finally, the performance of the proposed system is economically compared with the other previously proposed systems, i.e., those systems that take advantage of either solar energy or geothermal energy solely.

Fig. 1 Iran's solar radiation absorption potential (on a horizontal surface) and the geographical location of the case study

2 The case study

The proposed twofold system was employed to evaluate the thermal behavior of Dashte-Minoo greenhouse complex as the case study of this work. Dashte-Minoo greenhouse complex is located near Azadshahr City in the north-east of Iran with a latitude of 37° and longitude of 55°. According to Fig. 1, although Azadshahr City is in an area with the lowest amount of solar radiation absorption all over Iran, it is still an appropriate area to host greenhouses with an average daily irradiation of 4.5 kWh/m^2 day on a horizontal surface [24].

The case study includes ten similar greenhouses with the same dimensions, cultivating cucumber as its main crop for which the most suitable temperature is considered to be 20 °C [23]. The greenhouse cover material is also dual-layer polycarbonate with 8 mm thickness. Figure 2 presents information about the dimensions of each greenhouse in the case study.

Generally, in Iran, the heating demand of greenhouses is provided by diesel air heaters which burn natural gas. Figure 3 shows how the required heat of a greenhouse is provided in such a system. As the figure shows, the system takes advantage of an F.D. fan that intakes ambient air. This air then passes through an air heater burning natural gas which warms it up to the desired temperature. Afterward, the warmed air is distributed in the greenhouse space by secondary HVAC systems.

The energy balance on the above configuration may be written as:

$$\dot{Q}_{GR} = \dot{Q}_{lost} + \dot{Q}_{vent} - \dot{Q}_{solar}, \tag{1}$$

where $\dot{Q}_{GR}, \dot{Q}_{lost}, \dot{Q}_{vent}, \dot{Q}_{solar}$ are the required heat of greenhouse to stay at the desired temperature, the overall heat lost from the greenhouse to the environment and soil, the heat lost from the greenhouse due to ventilations and the absorbed solar energy into the greenhouse due to greenhouse effect, respectively. The overall heat loss from the greenhouse through the walls and field can be calculated by:

$$\dot{Q}_{lost} = \sum_{i=1}^{n} U_i A_i (T_{in} - T_a), \tag{2}$$

where U_i, A_i, T_a and T_{in} are, respectively, the overall heat transfer coefficient, the heat transfer area, the ambient temperature and the internal greenhouse temperature (20 °C) [23]. Table 1 details the values of U and A for the heat loss paths for each individual greenhouse.

The heat loss from the greenhouse due to the ventilation could also be obtained as:

$$\dot{Q}_{vent} = \frac{NV\rho c_p\ (T_{in} - T_a)}{3600}, \tag{3}$$

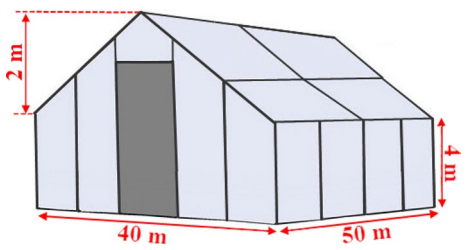

Fig. 2 The greenhouse dimensions of the case study

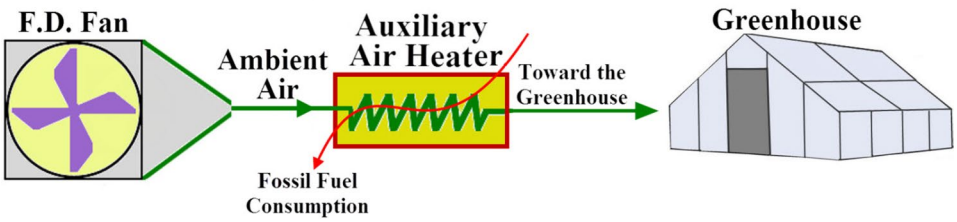

Fig. 3 The schematic diagram of heating preparation in greenhouses with a conventional configuration

Table 1 The values of U and A for the heat loss routs of each greenhouse

Loss path	A (m^2)	U (W/m^2 K)
Ceiling	2010	0.625
Southern and northern walls	200	0.625
Eastern and western walls	200	0.625
Field	2000	0.5

Table 2 The slope angle values for different walls of the greenhouse

Solar irradiation path	β
Southern	90
Ceiling	0
Eastern	90
Western	90

where c_p, ρ, V and N represent the constant pressure thermal capacity of air, the air density, the greenhouse volume and the greenhouse air change frequency during an hour (2 times per hour for winter and 20 times per hour for summer [23]), respectively. Finally, the absorbed solar heat in 1 m^2 area of each greenhouse due to the greenhouse effect is calculated as:

$$S = I_b R_b (\tau\alpha)_b + I_d (\tau\alpha)_d \left(\frac{1+\cos\ \beta}{2}\right) + I\ \rho_g (\tau\alpha)_g \left(\frac{1-\cos\ \beta}{2}\right), \quad (4)$$

where I, I_d, I_b and S are the total available solar radiation, the diffuse and beam components of solar radiation and the absorbed solar radiation, respectively. The Greek symbols β and $(\tau\alpha)$ also represent the surface tilt angle and the average absorption–transmission coefficient of the corresponding surface and its cover. Considering the greenhouse contents, the absorption coefficient for the internal elements of the greenhouse subjected to normal radiations is recommended to be 0.7 [23]. It is noteworthy here that the parameters S, I, I_b and I_d have the same unit (kJ/h m^2) and all of the other components in this equation are dimensionless. Detailed information about solar radiation calculation is available in [25–29]. Also, note that Eq. 4 must be employed to calculate the amount of solar energy entered and absorbed in the greenhouse from all sides except the northern wall of the greenhouse, as this wall is completely deviated from the south. Table 2 presents the values of β for all the walls and the ceiling of each greenhouse.

Finally, the total solar heat absorbed by the greenhouse internal elements could be calculated by:

$$\dot{Q}_{solar} = (S_{south} A_{south}) + (S_{east} A_{east}) + (S_{north} A_{north}) + (S_{west} A_{west}) + \left(S_{ceiling} A_{ceiling}\right). \quad (5)$$

Clearly, the unit of total absorbed solar heat is kJ/h. By calculating the heating demand of the greenhouse, one could then compute the amount of fuel consumption by the air heater as:

$$\dot{m}_f = \frac{\dot{Q}_{GR}}{LHV\ \eta_h}, \quad (6)$$

where η_h, LHV and $\dot{m}_f$ represent the air heater thermal efficiency, the fuel lower heating value and the fuel mass flow rate, respectively. In this work, the air heater thermal efficiency and consuming natural gas LHV are considered equal to 50 % and 48.1 MJ/kg, respectively [30, 31].

3 The proposed design

As the target temperature in the greenhouse is relatively low (20 °C), both of the renewable energy source systems proposed for this system are designed to provide low-temperature heat. Therefore, the employed solar collectors for the solar heater system are flat plate solar collectors and the boreholes in the geothermal heating system are supposed to be in middle range depths. Figure 4 illustrates the schematic diagram of the proposed system aimed at taking advantage of solar and geothermal energies simultaneously.

As the figure shows, the system takes advantage of three heat exchangers, i.e., the geothermal heat exchanger (GHE), the solar heat exchanger (SHE) and the auxiliary air heater (AAH). In fact, three cases are possible in the heating process. The first case is when the required heat is at very high levels due to the very low ambient temperature. In this case, all the three heaters should be employed to increase the air temperature up to the favorable value. For this objective, the intaken air by the F.D. fan enters the geothermal heat exchanger. The water within the geothermal heat exchanger receives the Earth's heat by passing through the geothermal boreholes and gives this heat back to the air stream. This air, then, enters the solar heat exchanger and its temperature goes up to higher values. Finally, the preheated air passes through the air heater to be heated up to the desired temperature.

The second possible case is when the ambient air can reach the desired temperature after passing through the geothermal and solar heat exchangers and, as a result, the air heater should be in standby mode. The dashed line parallel to the air heater is the path that the air should pass in this case.

Finally, the last case is when ambient temperature is in middle range (i.e., greater than 16 °C as the maximum possible geothermal boreholes outlet temperature and lower than 20 °C). Evidently, in this case, the geothermal

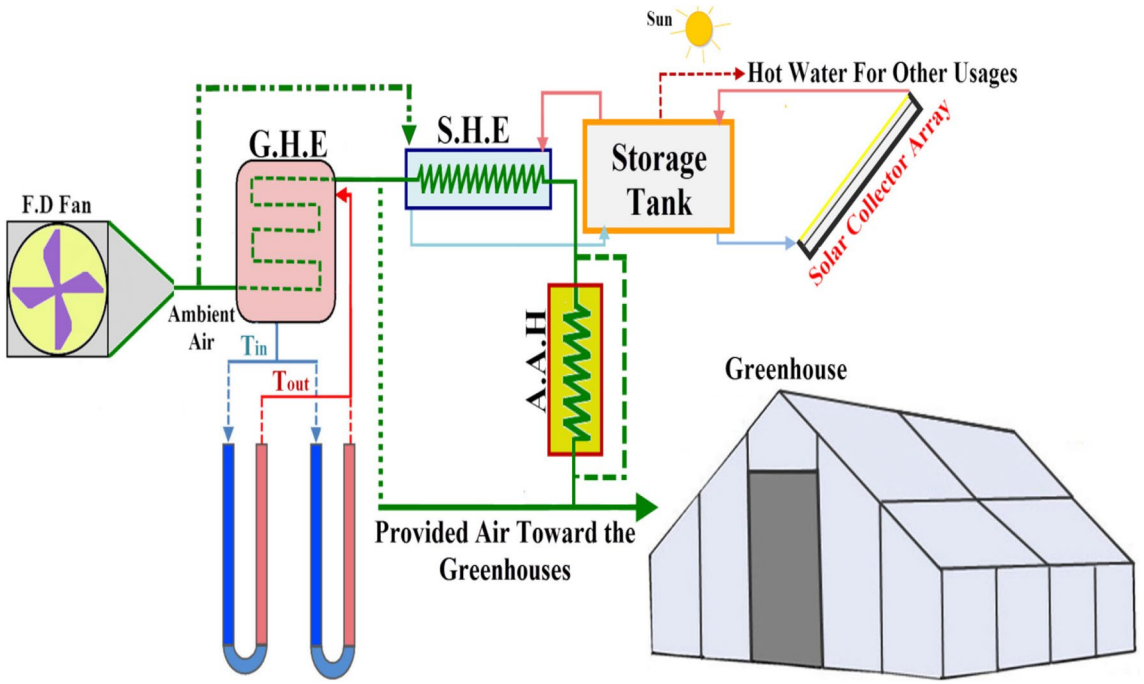

Fig. 4 The schematic diagram of proposed system to utilize simultaneous solar and geothermal energies in greenhouses

system could not be effective and the solar system solely provides the greenhouse heating demand. This issue will be explained thoroughly in the geothermal system formulation section. For this case, the solar heat exchanger is the only one that is used and the other two are in standby state.

3.1 The solar heater system details

There are a numbers of effective parameters on the performance of a solar heating system such as the type of collector employed, the tilt angle of collectors, the number of collector modules, the size of the solar storage tank and so on. As explained before, because low-temperature heat is required in greenhouses, flat plate collectors are employed in this work. Also, the previous study of the authors shows that the optimal slope angle of flat plate solar collectors for this area of Iran is 45° [23]. Table 3 presents detailed information about the solar heating system characteristics, resulting from a comprehensive thermo-economic analysis. The details of the data given by this table will be discussed in "Results".

Table 3 The proposed solar system details for the case study

The numbers of collectors	430
Collector slope angle	45°
Collector arrangement shape	Parallel
Storage tank volume	43 m^3
Operating fluid	Water
Operating fluid mass flow rate	12.9 kg/s
Collector length	200 cm
Collector wide	95 cm
Collector thickness	9.5 cm
Cover thickness	4 mm
Absorber plate thickness	0.5 mm
Tube inner diameter	10 mm
Tube outer diameter	12 mm
Tube space	150 mm
Plate area	1.51 m^2

3.2 The geothermal system details

For geothermal boreholes in middle depth ranges (up to 150 m), the maximum achievable temperature is equal to the annual average local ambient temperature which is 18.9 °C in the case study place [32]. Therefore, just for ambient temperatures lower than this value, the geothermal system could be employed for the heating task. For systems taking advantage of geothermal energy, there are a number of important issues to be considered in the simulation process, such as the number, depth and diameter of boreholes, the distance between the boreholes, operating fluid mass flow rate flowing through each borehole and the optimal volume of geothermal heat exchanger. Table 4 gives information about the characteristics of the geothermal heating unit in the proposed system resulting from the thermo-economic analysis accomplished on the system. The details of this analysis will also be presented in "Results".

Table 4 The proposed geothermal system details for the case study

The number of boreholes	35
Diameter of each borehole	0.15 m
Depth of each borehole	150 m
Distance between the boreholes	15 m
Borehole arrangement	Rectangular (5 × 7)
Operating fluid	Water
Operating fluid mass flow rate	0.14 kg/s
Operating fluid velocity	0.3 m/s
Pipe material	High density polyethylene
Pipe thermal conductivity coefficient	0.42 W/K
Pipe diameter	0.026 m
Pipe thickness	0.006 m
Grout thermal conductivity coefficient	1.25 W/K
Heat exchanger type	Shell and tube
Earth's temperature	18.9 °C
Earth's thermal conductivity coefficient	1.5 W/K
Earth's thermal diffusion coefficient	0.0778 m^2/day
Heat exchanger coil length	112 m
Heat exchanger coil diameter	0.1 m
Heat exchanger volume	12.5 m^3

3.3 Energy analysis of the proposed system

To analyze the thermal behavior of the system, four control volumes should be adopted and the first law of thermodynamics should be written for each one. The first control volume includes the geothermal heat exchanger and the boreholes for which the energy balance equation could be written as [25–29]:

$$m_{\mathrm{w}} c_{\mathrm{w}} \frac{\mathrm{d}T_{\mathrm{w}}}{\mathrm{d}t} = \dot{Q}_{\mathrm{GHX}} - \dot{Q}_{a-1}, \tag{7}$$

where m_{w}, c_{w} and T_{w} are the mass, specific heat capacity and temperature of the working fluid (water), respectively. Also, $\dot{Q}_{\mathrm{GHX}}$ and $\dot{Q}_{\mathrm{a-1}}$ refer to the absorbed heat from the earth by the operating fluid and the gained heat by the air intaken through the geothermal heat exchanger. It is noteworthy here that the boreholes are vertical types due to their higher efficiency and less requirement of space and energy for pumping the working fluid compared to the horizontal ones. The total heat absorbed by vertical boreholes could be given as [33]:

$$\dot{Q}_{\mathrm{GHX}} = q\, N_{\mathrm{bh}}\, H, \tag{8}$$

where N_{bh} and H are the number of boreholes and the effective length of each borehole, respectively. q is also the absorbable heat by one borehole individually for the unit effective length of the tube given by:

$$q = \frac{\dot{m}_{\mathrm{f}}\, c_{\mathrm{f}}\, (T_{\mathrm{out}} - T_{\mathrm{in}})}{H}, \tag{9}$$

in which $\dot{m}_{\mathrm{f}}$, c_{f}, T_{out} and T_{in} are the mass flow rate, thermal capacity, outlet temperature and inlet temperature of the working fluid, respectively. The value of T_{out} could be calculated as [33–36]:

$$T_{\mathrm{out}} = T_{\mathrm{gr}} + \left[\sum_{\lambda=1}^{n_t} \frac{q_\lambda - q_{\lambda-1}}{4\pi\, k_{gr}} \left(\int_{\frac{1}{\sqrt{4\alpha(t_\lambda - t_{\lambda-1})}}}^{\infty} I_e \frac{I_{ls}(\mathrm{HS},\ \mathrm{DS}')}{\mathrm{HS}'^2}\, \mathrm{dS}' \right) \right] + q R_{\mathrm{bh}} - \frac{qH}{2\dot{m}_{\mathrm{bh}} C_{\mathrm{bh}}}, \tag{10}$$

where λ again counts the hourly time steps, as all the calculation processes are mainly done on the basis of hourly periods. Therefore, q_λ represents the absorbed q in time step λ and $q_{\lambda-1}$ does that for time step λ−1. T_{gr}, k_{gr}, α also refer to the ground temperature, thermal conductivity coefficient and diffusion coefficient of the borehole, respectively. Defining S' as the Laplace transform variable in short-term response, $h = \mathrm{HS}'$, $d = \mathrm{DS}'$ and D as the ineffective length of tubes in the borehole, the other factors in Eq. 10 could be given by the following equations:

$$I_{\mathrm{ls}}(h,d) = 2\,\mathrm{ierf}(h) + 2\,\mathrm{ierf}(h+2d) - \mathrm{ierf}(2h+2d) - \mathrm{ierf}(2d), \tag{11}$$

$$\mathrm{ierf}(z) = z\mathrm{erf}(z) - \frac{1}{\sqrt{\pi}}\left(1 - e^{-z^2}\right); \quad \text{where : } \mathrm{erf}(z) = \frac{2}{\sqrt{\pi}} \int_0^z e^{-z^2}\mathrm{dz}. \tag{12}$$

The function I_{e} could also be given by:

$$I_{\mathrm{e}}(s) = \frac{1}{N} \sum_{i=1}^{N} \sum_{j=1}^{N} e^{-r_{ij}^2 S^2}, \tag{13}$$

where $r_{\mathrm{i,j}}$ represents the radial distance between borehole i and j ($i \neq j$). Also, R_{bh} in Eq. 10 is the overall thermal resistance of the borehole and could be obtained as:

$$R_{\mathrm{bh}} = \frac{1}{2}(R_{\mathrm{conv}} + R_{\mathrm{cond}}) + R_{\mathrm{grt}}, \tag{14}$$

in which the indices conv, cond and grt refer to the convectional heat resistance coefficient of the working fluid within the tubes, the conduction heat resistance coefficient of the tubes and the conduction heat resistance coefficient of the borehole walls given by the following three equations, respectively:

$$R_{\mathrm{conv}} = \frac{1}{\pi\, d_{\mathrm{i}}\, h_{\mathrm{f}}}, \tag{15}$$

$$R_{\mathrm{cond}} = \frac{\ln\left(d_{\mathrm{o}}/d_{\mathrm{i}}\right)}{2\,\pi\, k_{\mathrm{p}}}, \tag{16}$$

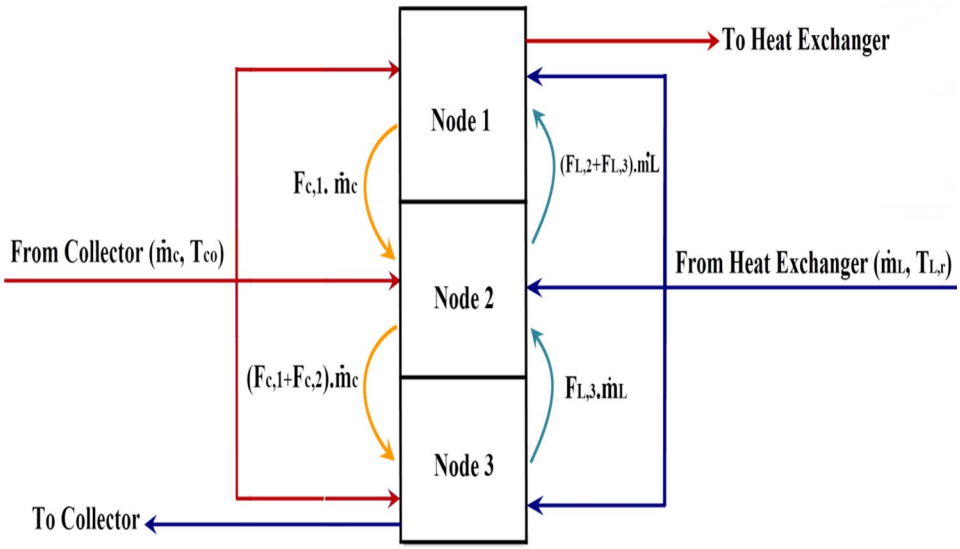

Fig. 5 The schematic of a three-node storage tank

$$R_{\mathrm{gr}} = \frac{1}{k_{\mathrm{gr}}\,\beta'_0\left(d_{\mathrm{b}}/d_o\right)^{\beta'_1}}, \tag{17}$$

where d_{i}, d_{o} and d_{bh} refer to the internal and external diameter of the tube and borehole diameter, respectively. h_{f}, k_{p} and k_{gr} also represent the convection and convective heat transfer coefficients for the fluid, the tube and the walls of the boreholes, respectively. β'_0 and β'_1 are also form factors reported in [33]. Finally, taking the above formulation into account and employing computational calculation methods (here, the modified version of Guadgk in Matlab), one could simulate the geothermal heating unit in the proposed system.

The second control volume is the solar heating heat exchanger. The first law of thermodynamics for this control volume could simply be written as:

$$m_w c_w \frac{\mathrm{d}T_w}{\mathrm{d}t} = \dot{Q}_{st} - \dot{Q}_{a-2}, \tag{18}$$

where $\dot{Q}_{\mathrm{st}}$ and $\dot{Q}_{\mathrm{a-1}}$ are the heat supplied to the heat exchanger by the solar storage tank and the heat given to the air stream passing through the heat exchanger. The third control volume in the system includes the collector modules as well as the solar storage tank. Evidently, the water density decreases as its temperature increases and, consequently, it comes up and lies in the upper levels of the storage tank. Therefore, to have an accurate simulation, the storage tank is considered as a multi-node tank instead of simply assuming a lumped control volume. Each node may then be considered as a lumped control volume. The number of nodes in a solar storage tank is recommended to be equal to 3 [24]. Figure 5 illustrates the schematic of a three-node storage tank.

The energy balance on each node of the storage tank can be written as:

$$\begin{aligned} m_{\mathrm{i}}\frac{\mathrm{d}T_{\mathrm{s,i}}}{\mathrm{d}t} &= \left(\frac{\mathrm{UA}}{c_{\mathrm{p}}}\right)_{\mathrm{i}}\left(T_{\mathrm{a}} - T_{\mathrm{s,i}}\right) + F_{\mathrm{i}}^{\mathrm{c}}\dot{m}_{\mathrm{c}}\left(T_{\mathrm{co}} - T_{\mathrm{s,i}}\right) \\ &+ \dot{Q}_{\mathrm{st}} + \begin{cases} \dot{m}_{\mathrm{m,i}}\left(T_{\mathrm{s,i-1}} - T_{\mathrm{s,i}}\right) & \text{if} \quad \dot{m}_{\mathrm{m,i}} > 0 \\ \dot{m}_{\mathrm{m,i+1}}\left(T_{\mathrm{s,i}} - T_{\mathrm{s,i+1}}\right) & \text{if} \quad \dot{m}_{\mathrm{m,i+1}} < 0 \end{cases} \end{aligned} \tag{19}$$

where T_{co}, $\dot{m}_{\mathrm{c}}$, T_{L}, T_o and $\dot{m}_{\mathrm{L}}$ are the temperature and mass flow rate of water entering the storage tank from the collectors' side, the temperature of water outgoing toward the solar heat exchanger and the collectors and the mass flow rate of water coming back from the solar heat exchanger. The function $F_{\mathrm{i}}^{\mathrm{c}}$ specifies which node receives the incoming hot water from the collectors' side.

$$F_{\mathrm{i}}^{\mathrm{c}} = \begin{cases} 1 \text{ if } \quad i = 1 \quad \text{and} \quad T_{\mathrm{co}} > T_{\mathrm{s,i}} \\ 1 \text{ if } \quad T_{\mathrm{s,i-1}} \geq T_{\mathrm{co}} > T_{\mathrm{s,i}} \\ 0 \text{ if } \quad i = 0 \quad \text{or if } i = N+1 \\ 0 \text{ otherwise} \end{cases}, \tag{20}$$

in which $T_{\mathrm{s,i}}$ is the temperature of node i. Also, the function $F_{\mathrm{i}}^{\mathrm{L}}$ determines which node receives the water coming back from the solar heat exchanger.

$$F_{\mathrm{i}}^{\mathrm{L}} = \begin{cases} 1 \text{ if } \quad i = 1 \quad \text{and} \quad T_{\mathrm{L,r}} > T_{\mathrm{s,i}} \\ 1 \text{ if } \quad T_{\mathrm{s,i-1}} \geq T_{\mathrm{L,r}} > T_{\mathrm{s,i}} \\ 0 \text{ if } \quad i = 0 \quad \text{or if } i = N+1 \\ 0 \text{ otherwise} \end{cases}. \tag{21}$$

Also, the water net mass flow rate between nodes $i-1$ and i can be given by:

$$\begin{cases} \dot{m}_{\mathrm{m,1}} = 0 \\ \dot{m}_{\mathrm{m},i} = \dot{m}_{\mathrm{c}}\sum_{\mathrm{j=1}}^{\mathrm{i-1}} F_{\mathrm{j}}^{\mathrm{c}} - \dot{m}_{\mathrm{L}}\sum_{\mathrm{j=i+1}}^{\mathrm{N}} F_{\mathrm{j}}^{\mathrm{L}} \\ \dot{m}_{\mathrm{m,N+1}} = 0 \end{cases} \tag{22}$$

Finally, $\dot{Q}_{st}$ in Eq. 19 is the rate of energy flowing from the storage tank into the heat exchanger and can be calculated by:

$$\dot{Q}_{st} = F_i^L \dot{m}_L \left(T_{L,r} - T_{s,i}\right). \tag{23}$$

On the other hand, the obtainable energy rate from a flat plate solar collector could be calculated by:

$$\dot{Q}_u = A_c F_R \left[S - U_l(T_{fi} - T_a)\right], \tag{24}$$

where F_R, T_{fi}, T_a, A_c and U_l are the collector removal factor, inlet working fluid temperature, ambient temperature, absorption surface area and the total heat transfer coefficient for the collector, respectively. Also, S is the absorbed solar flux by the flat plate collector per one square meter area and can be obtained from the equation below [24–29]:

$$S = I_T (\tau\alpha)_{av}, \tag{25}$$

where $(\tau\alpha)_{ave}$ and I_T are the average absorption–transmission coefficient of the collector and radiated solar flux on a tilted collector, respectively. It is noteworthy here that numerical methods are required for simulating the third control volume, and the Runge–Kutta method (for the storage tank) and Newton–Raphson method (for the collector modules) were employed in this work [23]. The last control volume in the system is the air heater and its heating duty could be calculated as follows:

$$\dot{Q}_{a-3} = \dot{Q}_{GR} - \dot{Q}_{a-1} + \dot{Q}_{a-2}, \tag{26}$$

where $\dot{Q}_{GR}$ is the total required heat of the greenhouse. Calculating the above equation, one could finally compute the amount of fuel consumption by the air heater as below:

$$\dot{m}_f = \frac{\dot{Q}_{a-3}}{\mathrm{LHV}\,\eta_h}. \tag{27}$$

4 Results

The only environmental parameter that affects the solar thermal system performance considerably is ambient temperature. For the geothermal system, however, besides ambient temperature, local ground temperature at the depth of 150 m, which is constant and equal to 18.9 °C in the case study location, is the effective parameter. The effects of other environmental factors, such as local humidity and air pressure, on the performance of the hybrid system are trifle and, as a result, their effects are neglected in this study. Figure 6 shows the local ambient temperature variation over 2013 in a monthly–hourly averaged format. As expected, the lowest and highest temperatures are observed in January and August, respectively. Note that, as it was explained, for temperatures over 20 °C (from early June to late August), the proposed system could not be effective enough, as the greenhouse heating demand is zero.

Figure 7 shows the total monthly heating demand of the whole greenhouse.

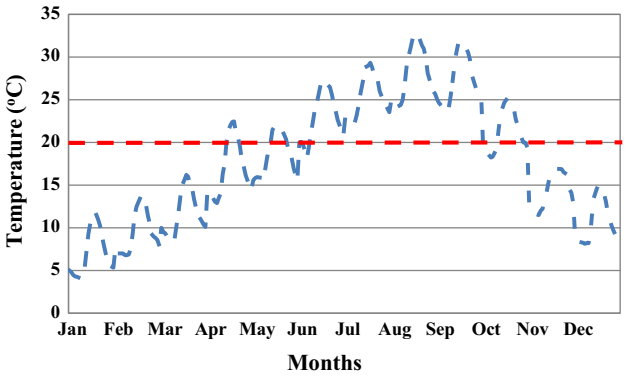

Fig. 6 The monthly–hourly averaged ambient temperature in 2013

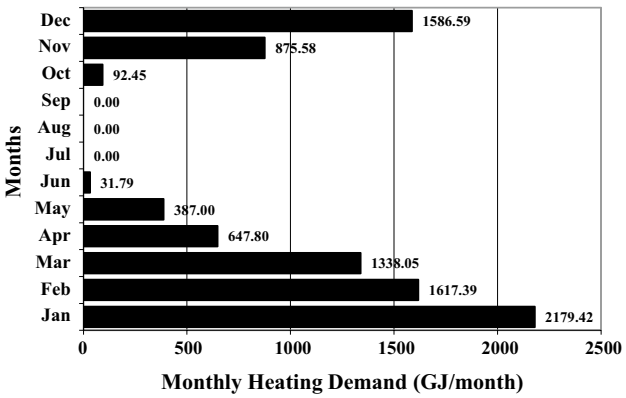

Fig. 7 The total monthly energy demand of the greenhouse in 2013

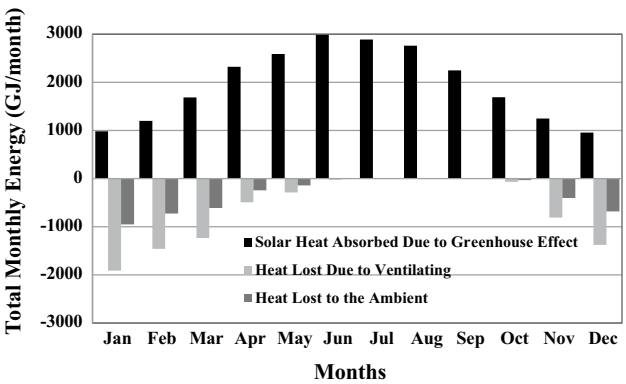

Fig. 8 The total monthly energy performance of the greenhouse in 2013

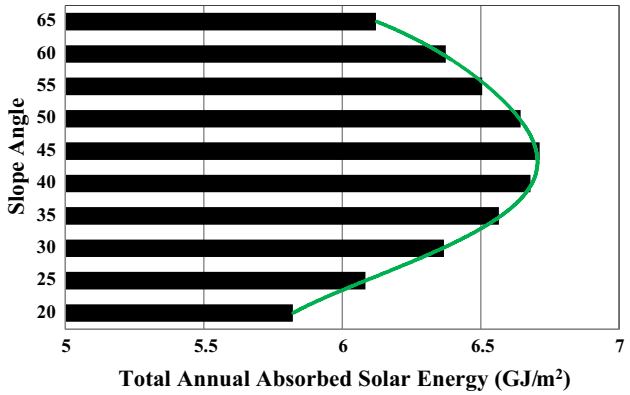

Fig. 9 The optimal slope angle determination

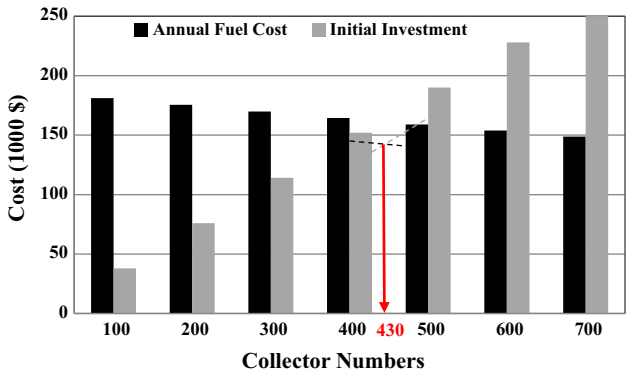

Fig. 11 The initial investment determination for the solar heater system

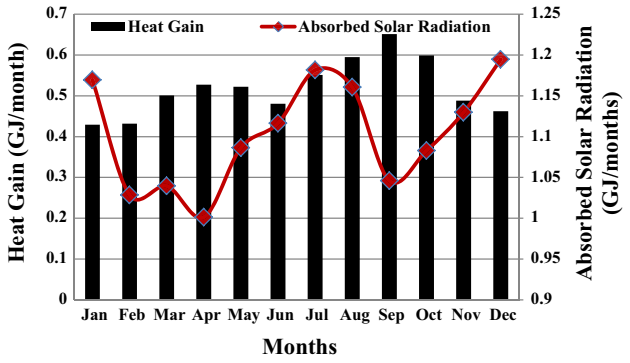

Fig. 10 The total monthly absorbed solar energy and heat gain by one collector

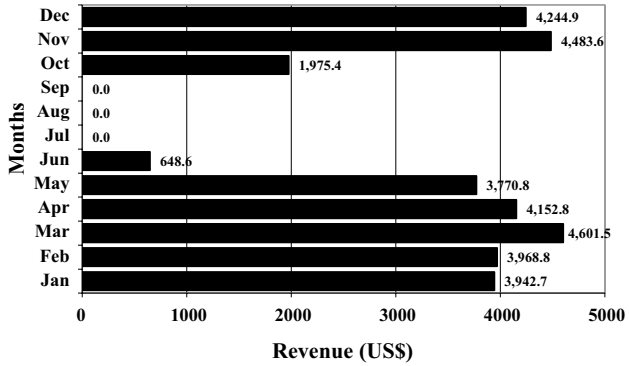

Fig. 12 The total monthly revenue in the case study by employing the proposed solar system only

Expectedly, the coldest month of the year coincides with the highest value of heating demand of the greenhouse and vice versa. The important note here is that although the ambient temperature during summer falls below 20 °C sometimes, the heating demand of the greenhouses is still zero in this period. This is certainly due to the greenhouse effect provided by the greenhouse covers.

Figure 8 shows the amount of various effective parameters contributing to the total energy demand of the greenhouse. Clearly, the absorbed heat must have positive values and heat losses should be reported as negative values.

Figure 9 shows how the solar collectors tilt affects the amount of absorbable solar irradiations over a whole year. Obviously, a surface sloped at 45 °C shows the best performance among all cases with a maximum absorbable solar radiation of 6.7 GJ/m^2 during the year.

Figure 10 presents information about the total monthly absorbed solar radiation and the useful energy delivered to the working fluid by one collector in the proposed system. According to the figure, the values corresponding to both of these parameters fluctuate sharply. Note that the considered slope angle is much more appropriate for winter rather than the optimal value of summer. As this factor is highly effective on the amount of absorbable solar energy, the maximum solar energy is absorbed in one of the coldest months of the year, i.e., December.

Based on the optimal initial investment determination approach thoroughly discussed in [36–38], the optimal solar system includes 430 flat plate collectors plus a storage tank with 43 m^3 volume. The cost of capital for this system is 163,000 US$. Figure 11 shows how this system came to be the most optimal system economically for the first step of modification in the greenhouse configuration, i.e., employing the solar thermal system.

It should be noted that the storage tank volume is proportional to the number of collectors (100 L for each collector), according to the previous study of the authors [32]. The consuming fuel of the air heater is considered to be natural gas of this area of Iran (Torkman gas), with a density of 0.578 kg/m^3 and LHV of 48.1 MJ/kg [37, 38]. The natural gas price has also been considered based on the current natural gas global price 0.25 US$/m^3. Also, the

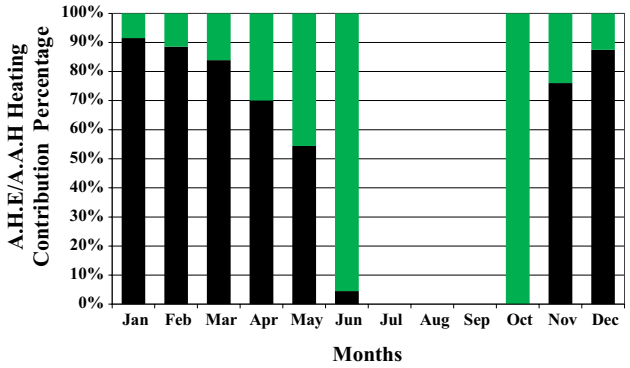

Fig. 13 The heating preparation contribution of AAH and SHE in the greenhouses equipped with only the solar heater system

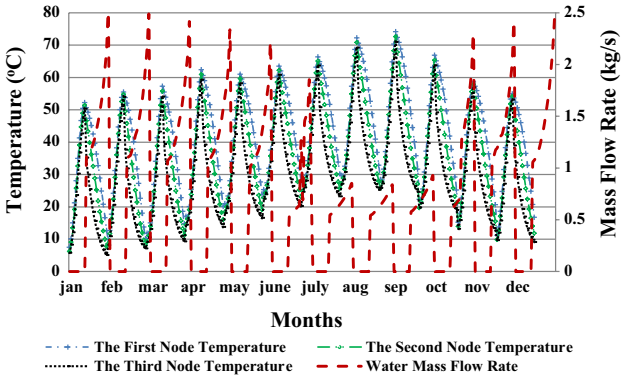

Fig. 14 Different node temperatures in the storage tank and the water mass flow rate

solar system cost including all its accessories is 380 US$/collector, and the seller company undertakes the whole installation process for free according to the purchase condition.

Figure 12 shows the total monthly revenue resulting from employing the proposed solar heating system in the case study. In terms of the net obtainable benefit, according to the figure, expectedly, during summer the obtainable benefit is zero as the air temperature is more than 20 and the highest amount of revenue is obtained in March. The total annual obtained revenue from the solar system equals 31,789.1 US$.

On the other hand, in terms of percentage of the required heat, the solar heating system shows the best and worst performance in October with almost 100 % and January with almost 8 % of the heating required, respectively. This issue is well shown in Fig. 13. Note that in this figure, the green area shows the contribution of solar heating system in the required heat preparation and the black area shows the diesel air heater contribution.

It is noteworthy here that in contrast to the constant water mass flow rate between the collectors and the storage tank during the energy storage step, the water mass flow rate between the storage tank and the solar heat exchanger is variable. This water is supposed to carry a constant rate of energy to the solar storage tank; therefore, as the temperature of the stored water decreases over the energy injection time, the mass flow rate should increase to the level of the energy support rate. Figure 14 shows the water mass flow rate between the storage tank and the solar heat exchanger as well as the temperature of each node in the storage tank in a monthly–hourly averaged format. In this figure, the mass flow rates equal to zero refer to sunshine hours in which the solar energy is supposed to be stored.

Expectedly, higher storage temperatures are reachable during summer, so that it rises up to about 75 °C in August and September. On the other hand, higher mass flow rates

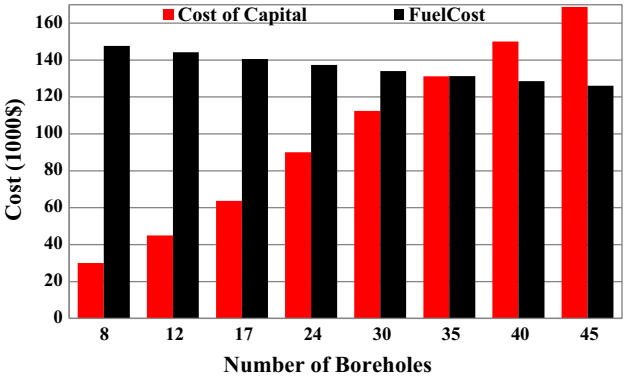

Fig. 15 Selecting the optimum number of boreholes in the proposed system

are required to supply the desired energy in the cold months of the year where water flow rate around 2.5 kg/s is sometimes required in both January and February.

The next step is presenting the details of analysis on the geothermal heating system. About the depth and the distance of boreholes, it is recommended to select the value of the BH factor (the ratio of the distances between the boreholes to the depth of each borehole) from 0.05 to 0.2 [33]. The cost of geothermal heating systems equipped to boreholes with depths up to 150 m is 25 US$/m in Iran, but this cost increases with the increase of borehole depth significantly. As low-temperature heat is required in the proposed system, boreholes with a depth of 150 m are considered in this work. Taking the value of BH considered and the boreholes' depths, the distance between the boreholes should be 15 m.

Also, for borehole diameter, generally, the smaller the diameter of a borehole, the higher is the heat transfer efficiency expected, and on the other hand, bigger diameters for the geothermal boreholes lead to bigger heat transfer area. Overall, the recommended diameter for geothermal

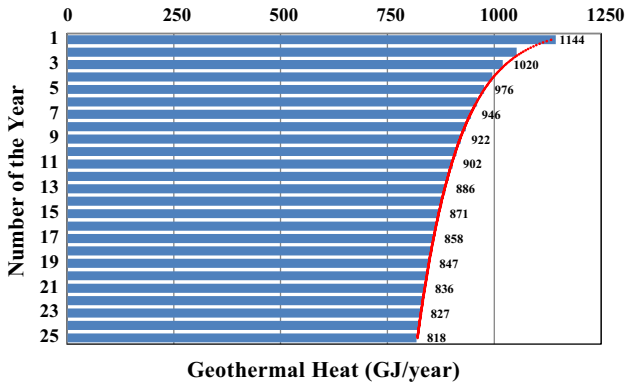

Fig. 16 The total annual obtainable heat from the geothermal system over time

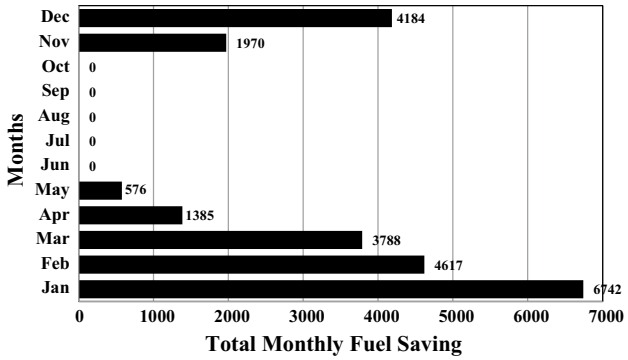

Fig. 17 The total monthly achievable benefit from the geothermal heating system through the first year

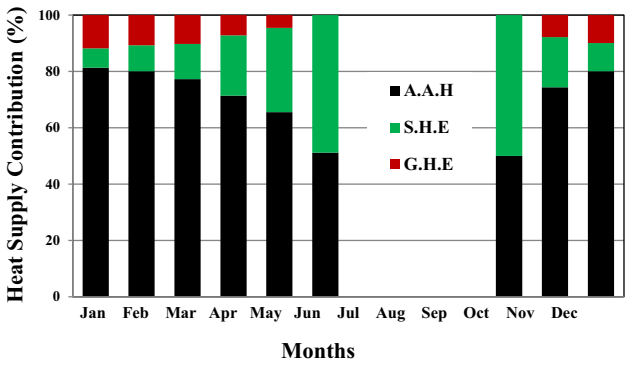

Fig. 18 The total monthly energy providing the contribution of each heater in the case study

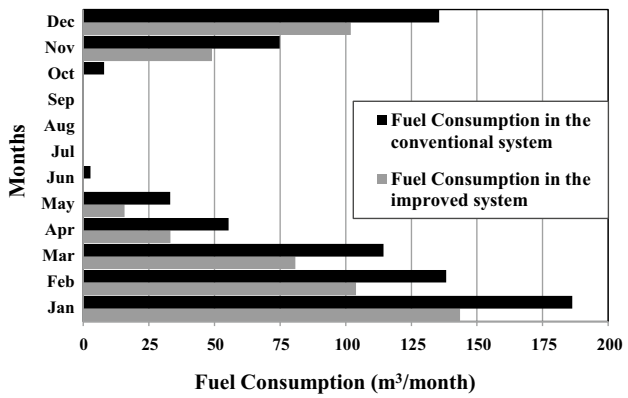

Fig. 19 Fuel consumption comparison between the proposed and conventional systems

boreholes is in the range of 90–190 mm [33]. The diameter of boreholes chosen for this work was 150 mm.

For selecting the optimal number of boreholes, which is a thermo-economical problem, a similar approach to the solar heating system optimum initial investment determination is used. Note that, here also, the capacity of the geothermal heat exchange is a functional of a number of boreholes (in this work, 0.5 m^3 for each borehole). Figure 15 shows how many boreholes should be hired in the proposed system. According to the figure, a geothermal system including 35 boreholes and a shell and tube heat exchanger with the capacity of 17.5 m^3 results in the best thermo-economical performance in the case study. It is worth mentioning that the recommended layout for geothermal boreholes is an L-shaped array; that is why, a rectangular 5 × 7 array has been considered for the boreholes in this work [33].

One should note that the expected lifetime of such geothermal systems is 25 years. Over time, the geothermal boreholes lose their efficiency little by little, so that the best achievable performance of the system is in the first year of its operation. Figure 16 shows the total annual obtainable heat by the proposed geothermal system.

As the figure shows, the total annual obtainable heat from the system in the first year is about 1144 GJ/year. As can be seen, although the total obtainable heat from the proposed geothermal heat decreases over time, it is still efficient enough at the end of the 25th year by over 818 GJ/year.

Figure 17 shows the total monthly benefit resulting from the geothermal system in the case study, taking the air heater efficiency, natural gas LHV and its universal price into account.

According to the figure, as the ambient air temperature is more than 16 °C during 5 months, the geothermal system does not lead to any revenue over this period. On the other hand, the best performance of the geothermal system is in January, more than 6700 US$ revenue, and overall, the total annual benefit resulting from employing this system in the first year equals to almost 24,000 US$.

Figure 18 shows the contribution of all heaters in the system (geothermal, solar and diesel heaters) in providing the required heat in each month of the year. Regarding the figure, in the cold months of the year, the contribution of

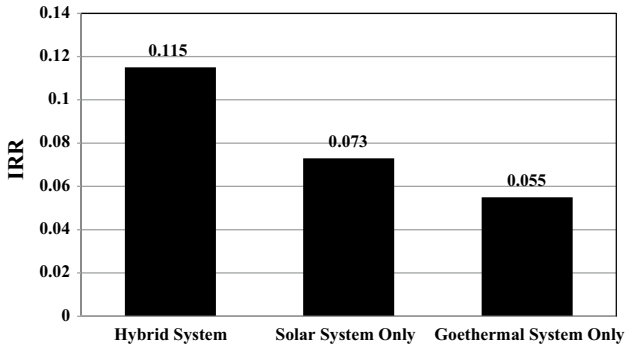

Fig. 20 IRR analysis results

the geothermal system rises, while in warmer months the solar system contribution in providing the required heat increases.

Figure 19 compares the total monthly fuel consumption of the greenhouses in the conventional and improved configurations.

This figure clearly shows how the proposed system is impressive in reducing the amount of fuel consumption in the case study. Obviously, the maximum fuel consumption reduction takes place in January, February and December by 42, 34 and 33 km^3 per month, respectively.

In the end, the IRR method is used to compare the performance of the hybrid proposed system in the case study with two more cases; (1) if the case study takes only advantage of the solar heating unit and (2) if the case study hires the geothermal system only. The IRR is the rate of return used to measure and compare the profitability of different projects. The IRR of a project is the rate of return by which the net present value (NPV) of all cash flows of an investment equals zero. The NPV could be calculated as:

$$\mathrm{NPV} = \sum_{\mathrm{t}=1}^{\mathrm{N}} \frac{R_{\mathrm{t}}}{(1+i)^{\mathrm{t}}}, \tag{28}$$

where I, t and R_{t} represent the interest rate, the time of cash flow and the net cash flow in the project, respectively [33]. Overall, the higher values of IRR in a project make it more appropriate to be implemented [24, 33]. The critical parameter for calculating the IRR of a project is the number of years during which the NPV equals zero. For such industrial projects, the duration of 8 years seems to be a good choice. Figure 20 shows the results of the IRR analysis.

As the figure proves, the best economical performance with a significant superiority relative to the other two systems is related to the hybrid system proposed with an IRR equal to 0.115. As the figure shows, the system equipped to the solar heating system only shows the second best performance with an IRR of 0.073, while the worst performance is presented by the system equipped with the geothermal heating unit with an IRR of only 0.055. Note that in the figure above, the total retaining and maintenance costs of both solar and geothermal systems have been considered equal to 5 % of the total capital cost of each one.

5 Conclusion

There are many places in the industry which have high potential to be equipped with renewable energy systems to modify their fuel usage pattern. A huge amount of fossil fuel is burnt in greenhouses all around the world every year. This work shows how employing a hybrid system taking advantage of geothermal and solar heating systems can considerably improve the fuel consumption pattern of a sample greenhouse in Iran. The proposed system employs 430 flat plate collectors and a solar storage tank with 43 m^3 volume plus a geothermal system including 35 boreholes and a shell and tube heat exchanger with 17.5 m^3 volume. The total cost of the proposed system is 294,000 US$ and with an IRR of 0.115. Also, the economic performance of the proposed hybrid system was compared with two other systems, i.e. a greenhouse taking advantage of solar energy only and another greenhouse that utilizes geothermal energy only, and it was shown that the proposed system was considerably more efficient than the other two systems. Also, considering that the typical greenhouse of this work is located in the north of Iran with a moderate climate, the proposed system can even be more efficient for the central area of Iran with a much warmer weather. Therefore, taking the results of this study into account, employing the proposed hybrid system in greenhouses is highly recommended.

References

1. Ejilah R, Abdulkadir L, Adisa B (2012) Review of *Sclerocarya birrea* seed oil extracted as a bio-energy resource for compression ignition engines. Int J Agric Biol Eng 5(3):1–9
2. Canakci M, Akinci I (2006) Energy use pattern analyses of greenhouse vegetable production. Energy. 31:1243–1256
3. Heidari MD, Omid M (2011) Energy use patterns and econometric models of major greenhouse vegetable productions in Iran. Energy 36:220–225
4. Omid M, Ghojabeige F, Ahmadi F, Delshad F (2011) Energy use pattern and bench-marking of selected greenhouses in Iran using data envelopment analysis. Energy Convers Manag 52:153–162
5. Hatirli SA, Ozkan B, Fert C (2006) Energy inputs and crop yield relationship in greenhouse tomato production. Renew Energy 31:427–438
6. Ozkan B, Ceylan RF, Kizilay H (2011) Energy inputs and crop yield relationships in greenhouse winter crop tomato production. Renew Energy 36:3217–3221
7. Tzempelikos A, Athienitis AK (2007) The impact of shading design and control on building cooling and lighting demand. Sol Energy 81(3):369–382

8. Vadiee Amir, Martin Viktoria (2013) Thermal energy storage strategies for effective closed greenhouse design. Appl Energy 109:337–343
9. Zhang Y, Gauthier L, Halleux DD, Dansereau B, Gosselin A (1996) Effect of covering materials on energy consumption and greenhouse microclimate. Agric For Meteorol 82:227–244
10. Cossu Marco, Murgia Lelia, Ledda Luigi, Deligios Paola A, Sirigu Antonella, Chessa Francesco, Pazzona Antonio (2014) Solar radiation distribution inside a greenhouse with south-oriented photovoltaic roofs and effects on crop productivity. Appl Energy 133:89–100
11. Willits DH, Chandra P, Peet MM (1985) Modelling solar energy storage systems for greenhouses. J Agric Eng Res 32(1):73–93
12. Liu T, McConkey B, Huffman T, Smith S, MacGregor B, Yemshanov D, Kulshreshtha S (2014) Potential and impacts of renewable energy production from agricultural biomass in Canada. Appl Energy 130:222–229
13. Abdel-Ghany AM, Al-Helal IM (2011) Solar energy utilization by a greenhouse: general relations. Renew Energy 36(1):189–196
14. Lazaar M, Kooli S, Hazarni M, Farhat A, Belghith A (2004) Use of solar energy for the agricultural greenhouses autonomous conditioning. Desalination 168:169–175
15. Vadiee Amir, Martin Viktoria (2013) Energy analysis and thermo-economic assessment of the closed greenhouse—the largest commercial solar building. Appl Energy 102:1256–1266
16. Rafferty K (1986) Some considerations for the heating of greenhouses with geothermal energy. Geothermics 15(2):227–244
17. Bakos GC, Fidanidis D, Tsagas NF (1999) Greenhouse heating using geothermal energy. Geothermics 28(6):759–765
18. Karytsas C (2003) 03/01823 Low enthalpy geothermal energy utilisation schemes for Greenhouse and district heating at Traianoupolis Evros, Greece, Fuel and energy abstracts, vol 44, issue 5, p 311
19. Ghosal MK, Tiwari GN (2004) Mathematical modelling for greenhouse heating by using thermal curtain and geothermal energy. Sol Energy 76(5):603–613
20. von Zabeltitz C (1986) Greenhouse heating with solar energy. Energy Agric 5(2):111–120
21. Kürklü Ahmet, Bilgin Sefai, Özkan Burhan (2003) A study on the solar energy storing rock-bed to heat a polyethylene tunnel type greenhouse. Renew Energy 28(5):683–697
22. Xu J, Li Y, Wang RZ, Liu W (2014) Performance investigation of a solar heating system with underground seasonal energy storage for greenhouse application. Energy 67(1):63–73
23. Farzaneh-Gord M, Arabkoohsar A, Deymi-Dashtebayaz M, Khoshnevis AB (2013) New method of solar energy application in greenhouses in order to decrease fuel consumption. Int J Agric Biol Eng 6(4):64–75
24. Farzaneh-Gord M, Arabkoohsar A, Deymi-Dashtebayaz M, Machado L, Koury RNN (2014) Energy and exergy analysis of natural gas pressure reduction points equipped with solar heat and controllable heaters. Renew Energy 72:258–270
25. Farzaneh-Gord M, Arabkoohsar M, Deymi-Dashtebayaz M, Farzaneh-Kord V (2012) Feasibility of accompanying uncontrolled linear heater with solar system in natural gas pressure drop stations. Energy 41:420–428
26. Farzaneh-Gord M, Arabkoohsar A, Rezaei M, Deymi-Dashtebayaz M (2011) Feasibility of employing solar energy in natural gas pressure drop stations. J Energy Inst 84(3):165–173
27. Arabkoohsar A, Farzaneh-Gord M, Deymi-Dashtebayaz M, Machado L, Koury RNN (2015) A new design for natural gas pressure reduction points by employing a turbo expander and a solar heating set. Renew Energy 81:239–250
28. Arabkoohsar A, Machado L, Farzaneh-Gord M, Koury RNN (2015) The first and second law analysis of a grid connected photovoltaic plant equipped with a compressed air energy storage unit. Energy 87:520–539
29. Arabkoohsar A, Machado L, Farzaneh-Gord M, Koury RNN (2015) Thermo-economic analysis and sizing of a PV plant equipped with a compressed air energy storage system. Renew Energy 83:491–509
30. Farzaneh-Gord M, Parvizi S, Arabkoohsar A, Machado L, Koury RNN (2015) Potential use of capillary tube thermal mass flow meters to measure residential natural gas consumption. J Nat Gas Sci Eng 22:540–550
31. Deymi-Dashtebayaz M, Farzaneh-Gord M, Arabkoohsar A, Khoshnevis AB, Akeififar H (2014) Improving Khangiran gas turbine efficiency by two standard and one novel inlet air cooling method. J Braz Soc Mech Sci Eng 36(3):571–582
32. https://eosweb.larc.nasa.gov/cgi-bin/sse/retscreen.cgi?email=skip@larc.nasa.gov. Accessed 14 Dec 2015
33. Farzaneh-Gord M, Ghezelbash R, Arabkoohsar A, Pilevari L, Machado L, Koury RNN (2015) Employing geothermal heat exchanger in natural gas pressure drop station in order to decrease fuel consumption. Energy 83(1):164–176
34. McKibbin R (1998) Mathematical models for heat and mass transport in geothermal systems. Transport phenomena in porous media, p 131–154
35. Bahadori Alireza, Zendehboudi Sohrab, Zahedi Gholamreza (2013) A review of geothermal energy resources in Australia: current status and prospects. Renew Sustain Energy Rev 21:29–34
36. Østergaard PA, Lund H (2011) A renewable energy system in Frederikshavn using low-temperature geothermal energy for district heating. Appl Energy 88(2):479–487
37. Farzaneh-Gord M, Farsiani M, Khosravi A, Arabkoohsar A, Dashti F (2015) A novel method for calculating natural gas density based on Joule Thomson coefficient. J Nat Gas Sci Eng 26:1018–1029
38. Farzaneh-Gord M, Arabkoohsar A, Koury RNN (2016) Novel natural gas molecular weight calculator equation as a functional of only temperature, pressure and sound speed. J Nat Gas Sci Eng 30:195–204